


Article

Influence of Failure Probability Due to Parameter and Anchor Variance of a Freeway Dip Slope Slide—A Case Study in Taiwan [†]

Shong-Loong Chen and Chia-Pang Cheng * 

Department of Civil Engineering, National Taipei University of Technology, Taipei 10608, Taiwan; f10391@ntut.edu.tw

* Correspondence: cheng.jiabang@gmail.com; Tel.: +886-2-8969-1900

[†] This paper is an extended version of our papers published in the International Conference on Recent Trends in Engineering Science and Management, New Delhi, India, 15 March 2015 and the 4th GeoChina International Conference on Sustainable Civil Infrastructures: Innovative Technologies for Severe Weathers and Climate Changes, Shandong, China, 25–27 July 2016 (With permission from ASCE).

Received: 19 June 2017; Accepted: 18 August 2017; Published: 22 August 2017

Abstract: The traditional slope stability analysis used the Factor of Safety (*FS*) from the Limit Equilibrium Theory as the determinant. If the *FS* was greater than 1, it was considered as “safe” and variables or parameters of uncertainty in the analysis model were not considered. The objective of research was to analyze the stability of natural slope, in consideration of characteristics of rock layers and the variability of pre-stressing force. By sensitivity and uncertainty analysis, the result showed the sensitivity for pre-stressing force of rock anchor was significantly smaller than the cohesive (*c*) of rock layer and the varying influence of the friction angle (ϕ) in rock layers. In addition, the immersion by water at the natural slope would weaken the rock layers, in which the cohesion *c* was reduced to 6 kPa and the friction angle ϕ was decreased below 14° , and it started to show instability and failure in the balance as *FS* became smaller than 1. The failure rate to the slope could be as high as 50%. By stabilizing with a rock anchor, the failure rate could be reduced below 3%, greatly improving the stability and the reliability of the slope.

Keywords: slope; factor of safety; sensitivity; uncertainty; cohesive; friction angle

1. Introduction

Landslides, earthquakes, floods and typhoons are the four major natural disasters that have caused property damage and loss of life in the world, especially in Taiwan. Taiwan is located in the Pacific tropical region, located in the Pacific coast seismic belt, suffered typhoons, heavy rain, drought, cold, earthquake and other natural disasters, an average of about three to four typhoons each year to attack Taiwan, and the scale of more than five earthquakes at an average of 24.4. Thus, landslide prevention is an important issue.

Traditional slope analysis and design is based on a deterministic approach that uses a static limit equilibrium analysis to assess the factor of safety (*FS*), which is calculated by dividing the resisting forces by the driving forces [1]. If the *FS* was greater than 1, it is considered “safe”; in other words, the *FS* being less than 1 is considered “failure”. However, the single deterministic *FS* of a slope is often not enough to analyze the slope stability due to uncertainty in input parameters. Slope stability assessment and *FS* calculations involve many variables, such as cohesive, friction angle, anchor force, unit weight, water pressure, and seismic acceleration, etc. Limit equilibrium analysis that uses a single value for each variable to mathematically determine the *FS* cannot quantify the slope failure

probability. This is because slopes with equivalent FS values may nonetheless have different risks of failure depending on variations in their soil properties [2,3].

The probabilistic approach feature takes into account the influence of the uncertainty of all parameters. The method consists of obtaining the mean and standard deviation parameters, calculating the probability distribution of the FS , and assessing the slope failure probability (P_f). Probability analysis was first developed in the 1940s and used for the first time in slope engineering in the 1970s [4–10]. In recent years, due to the dramatic changes in the climate, environmental changes have gradually increased, landslide analysis of the external and internal environmental parameters has increased the uncertainty [11], and more and more scholars of slope stability analysis and research use probabilistic techniques [12–19]. Probability analysis is applied to slope stability analysis, collecting relevant literature, often using methods as follows: (1) First and Second Order Reliability Methods (FORM and SORM) or First Order Second Moment Method (FOSM) [20–22]; (2) Response Surface Method (RSM) [23–25]; (3) Subset Simulation [13,25,26]; (4) Stochastic Collocation (SC) [27,28]; (5) Quadrature Method of Moments (QMOM) [29,30]; (6) Monte Carlo simulations (MCS) [25,31–35]; and (7) Point Estimate Method (PEM) [36–41].

In general, all of the above methods have various benefits and drawbacks with respect to their accuracy, numerical efficiency, and range of applications. The first-order second-moment (FOSM) method or the Second Order Second Moment (SOSM) method are probabilistic approaches to determine the statistical moment of a function with stochastic input variables. The name is based on the derivation, which uses a first-order Taylor series along with the first and second moments of the input variables. FOSM methods lack the capacity, however, to handle nonlinear models and non-normal stochastic variables, a shortcoming which likely results in miscalculations. The Response Surface Method (RSM), meanwhile, consists of a collection of mathematical and statistical techniques that can be used for empirical model building, which explores the relationships between several explanatory variables and one or more response variables. Whether SORM, FORM or RSM are used, these approaches all use the moments of performance function to compute the failure probability, meaning that all of these approaches are approximate methods. As such, a more accurate, reliable, and effective method of calculation would be highly valuable. This is the reason why MCS has come into being. Given the probability distribution of a group of independent stochastic variables, the MCS can be used to calculate a slope's failure probability according to the assumed probability distribution of dependent stochastic variables. MCS benefits of this method are offered a conceptually easily understood and robust method to assess the system failure probability of slope stability, especially in spatially variable rocks.

The basic idea of PE is to use sample data to compute a single value (called a statistic), which then serves, in turn, as a “best estimate” or “best guess” value for an unknown population parameter (whether fixed or random). Although the PE differs from the MCS in that it does not furnish directly a full distribution of the output variable, it can be used without substantial knowledge regarding probability concepts and can also be used for any probability distribution. As such, it may be used quite commonly in the future for reliability analyses and to evaluate engineering systems for failure probability.

This paper used the dip-slope failure at the 3.1 K section of Taiwan's Formosa Freeway (Freeway No. 3) as a case study. The aim of the study was to provide a slope model that would be consistent with the actual field conditions in order to investigate slope factor of safety variations and variations in rock slope parameters (c , ϕ) and anchor force (T) both prior to and after the weakening and immersion of slope rocks. First, we used the sensitivity analysis to explore the impact of the uncertainty or variability of the input parameter values on the FS . Secondly, three different PEMs (RPEM, HPEM and MPEM) were used to study how parameter uncertainty impacted slope stability. MCS was used to check the accuracy. Finally, the influence of the correlation coefficient between c and ϕ on the factor of safety is discussed.

2. Case Description and Performance Function

2.1. Overview of the Dip Slope Slides on National Freeway No. 3 in Taiwan

Taiwan's Formosa Freeway, also known as Freeway No. 3, is the second of the island's major North–South freeways. On 25 April 2010, around 2 p.m., a landslide occurred on the right side slope in the southbound 3.1 km section of the National Freeway No. 3 in Cidu. The landslide occurred in a second and buried both directions of the freeway about 190 m. This landslide was due to the sliding of a wedge-shape sandstone slope that lies beneath both the National Freeway No. 3 and highway 62. The sliding distance was about 70–80 m (see Figure 1). There were several days without rain fall before the landslide, but abundant water still could be found on the sliding surface, which implies that the underground water played an important role in this landslide. In this landslide, at least four people were killed, three cars were buried, and a bridge was destroyed [42,43].



Figure 1. Large-scale landslides on a dip slope on the Taiwan Formosan Freeway.

The rocks in the area are sedimentary rocks, and come from a sandstone section (SS) located at the bottom of the Miocene Shihti Formation (St). The thickness of this SS is roughly 15 to 20 m. Figure 2 consists of a geological map of the area and shows that the terrain in the area is essentially a sedimentary rock formation consisting of alternating sections of sandstone and shale. The shear strength parameters of the rocks in the location of the dip slope slide in the southbound 3.1 km of the National Freeway No. 3 in Cidu are listed in Table 1. The four rows denoted by light red are the critical layer. This layer was identified to be the layer that contains the actual failure surface.

Table 2 shows the original design parameters and Figure 3 shows that there are six primary layers making up the geological profile of the slope. The top layer consists of a 2–5 m thick overburden, while the second layer of sandstone (SS) has a thickness of approximately 10 m. The third layer consists of a 1-m thick layer of alternating sandstone and shale (SS/SH), while the fourth layer consists of dark gray shale (SH) approximately 6 m thick. Sandstone comprises both the fifth and sixth layers, each of which is about 2–3 m thick. The sliding plane was located close to the interface between the third layer and the top of the fourth layer consisting of dark gray shale. A clay seams that are considered to be potential causes of tilt failure are found at the same depth as the sliding plane in some of the boreholes. The design of the excavated dip slope consisted of three tiers with 1:1–1:1.5 slopes. Each of these three tiers was reinforced with ground anchors with a horizontal spacing of 2.6 m and an anchor load of 60 t each.



Figure 2. The regional geological map at Taiwan Formosan Freeway.

Table 1. Shear strength parameters [43].

No.	Hole No.	Depth (m)	Peak Strength		Residual Strength	
			C_p (kg/cm ²)	ϕ_p (°)	C_r (kg/cm ²)	ϕ_r (°)
RDS(D)-1	B-1	3.00–4.00	2.5	28.0	0.0	25.0
RDS(D)-2	B-2	4.00–5.00	2.6	30.1	0.0	28.0
RDS(D)-3	B-4	2.60–3.60	1.5	26.7	0.0	22.0
RDS(D)-4	B-6	16.60–17.00	0.28	22.5	0.0	19.8
RDS(D)-5	B-7	18.00–19.00	3.2	28.5	0.0	22.7
RDS(D)-6	B-8	16.00–17.00	0.7	36.5	0.0	29.0
RDS(W)-1	B-1	0.00–1.00	2.1	29.0	0.0	17.2
RDS(W)-2	B-2	3.40–3.80	0.5	46.0	0.0	22.0
RDS(W)-3	B-3	16.60–17.00	0.9	27.7	0.0	23.2
RDS(W)-4	B-5	16.60–17.00	1.1	26.2	0.0	14.1
RDS(W)-5	B-9	38.00–39.00	0.5	34.6	0.0	21.0
RDS(W)-6	B-10	10.25–11.00	1.4	37.0	0.0	24.6
RDS(W)-7	B-6	22.40–22.50	-	-	0.0	21.5
RDS(W)-8	B-6	17.30–17.40	-	-	0.0	20.0

RDS: Rock Direct Shear test.

Table 2. Design parameters [43].

	Layer	Depth (m)	γ_t (kN/m ³)	γ_{sat} (kN/m ³)	c (kPa)	ϕ (°)
1	sandstone (SS)	5–20	21	21	30	32
2	sandstone and shale (SS/SH)	2	21	21	10	20
3	shale (SH)		21	21	30	28

The case of the disaster is mainly and typically slope sliding. According to the characteristics of the disaster, the sliding surface of the sliding slope is weakened by the groundwater infiltration. The slope will reach a critical condition and rock anchor components have an obvious corrosion phenomenon, and will gradually reduce the tensile strength of anchor and slope factor of safety, but also cause the slope system to fail in a short time.

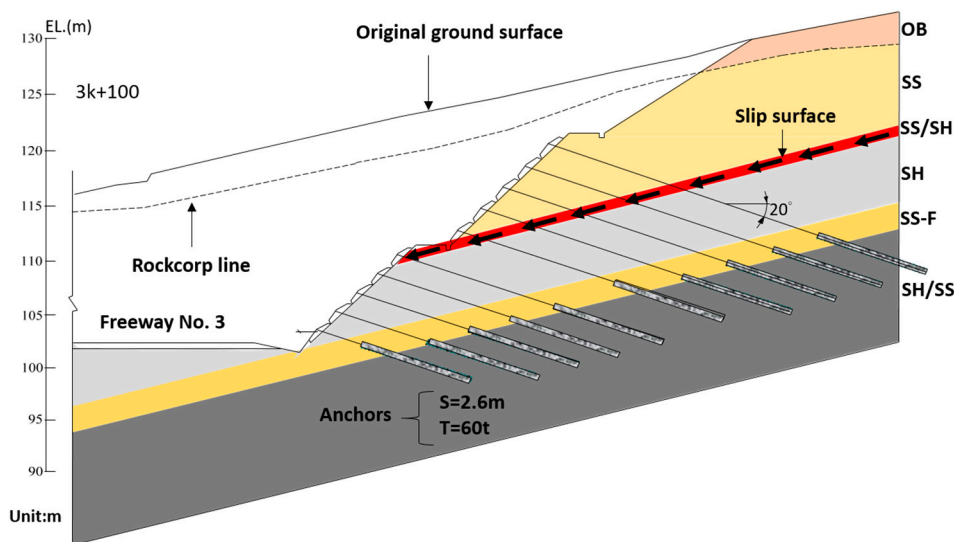


Figure 3. Geological profile and geometry of a cross-section of the slope on the Taiwan Formosan Freeway.

2.2. Performance Function

The landslide at the 3.1 K section of the Taiwan Formosa Freeway was a dip-slope slide caused by the sliding of the sand-shale strata. The precise location of the slip surface, which, as indicated in Figure 4, can be viewed in simplified terms as a single plane failure surface, was ascertained via a site investigation. An analysis of the rock slope stability could then be obtained through the use of a deterministic model [44]. The fundamental cause of the failure was that an unstable block of weight (W) was resting on a plane surface that was inclined at a θ angle to the horizontal. The force of gravity caused the block to try to move along the joint plane AC. Using the limit equilibrium method, the factor of safety (FS) in this context would be defined as the ratio of shear strength to shear stress [2,3].

$$FS = \frac{\text{Resistance}}{\text{Driving force}} = \frac{2c \sin \beta}{rH \sin(\beta - \theta) \sin \theta} + \frac{\tan \phi}{\tan \beta} + \frac{2T \cos(\theta + \delta) \sin \beta}{rH^2 \sin(\beta - \theta)s}, \quad (1)$$

$$\text{Probability of failure } P_f = \Pr(FS \leq 1), \quad (2)$$

where the interface parameters of shear strength are c and ϕ , the weight of the sliding wedge ΔABC is W , the unit weight of rock is r , the height of slope is H , the length of the sliding surface is L , the inclination of the sliding surface is θ , and the normal force acting on the sliding surface is N . Furthermore, T is the rock anchoring force, δ is set to play rock anchor angle, s is the horizontal spacing of anchor.

appropriate to use the method for the treatment of stochastic variables that are symmetric. For problems involving only a single stochastic variable, HPEM is identical to the RPEM with a zero skew coefficient. The theoretical basis of HPEM is built on orthogonal transformation using eigenvalue decomposition. Further explanations of HPEM can be found in [4,9–11].

3.1.3. Modified Harr Point Estimate Method (MPEM)

Chang [45] proposes an alternative PEM to avoid the computational drawbacks described above for the two existing PEMs (RPEM and HPEM). It should be noted that, for the model involving the multiplication of stochastic parameters with normal distributions, the accuracy of the three PE methods was found to be rapidly decreased as the order of moments and the number of stochastic parameters were increased. Compared to its competitors, however, the MPEM produces estimates of the moments for model output that are more accurate, particularly under circumstances in which the number of stochastic parameters is not excessively high.

In a range of the cases examined, meanwhile, use of statistical moments alone as a basis for comparison fails to yield a clear picture of how well the three PEMs perform relative to each other. Therefore, the moments obtained from the MCS were used to create a specified distribution that the statistical moments estimated by the PEMs could then be incorporated into in order to compare how close their distribution curves were to the actual data as determined by the MCS.

The goodness-of-fit of any two distribution curves was evaluated using three criteria. When the number of stochastic parameters was large and the first two moments only were considered, and when normal and lognormal distributions were assumed for the two nonlinear model outputs, the MPEM was less accurate than the other two PE methods. However, the accuracy of the MPEM was significantly improved by the further incorporation of skew coefficients.

Figure 5 shows the differences in point selection in the standardized parameter space when the three PEMs are used for a bivariate case. The RPEM is located at the corner of the square with the original length as the center, and the side length is 2. However, the eigenvector of the bivariate correlation matrix is 45° from the axis of each normalized parameter. Therefore, the HPEM selects the points of intersection between the eigenvectors and the circle with the radius of $n^{0.5}$ centered at the origin, which were the same points selected by the RPEM in the case of bivariate. It should be noted, meanwhile, that the points selected by the MPEM are elliptical contours of equal density, which are circles in the normalized eigen-space. When the stochastic variable is not relevant, the proposed MPEM is the same as the HPEM.

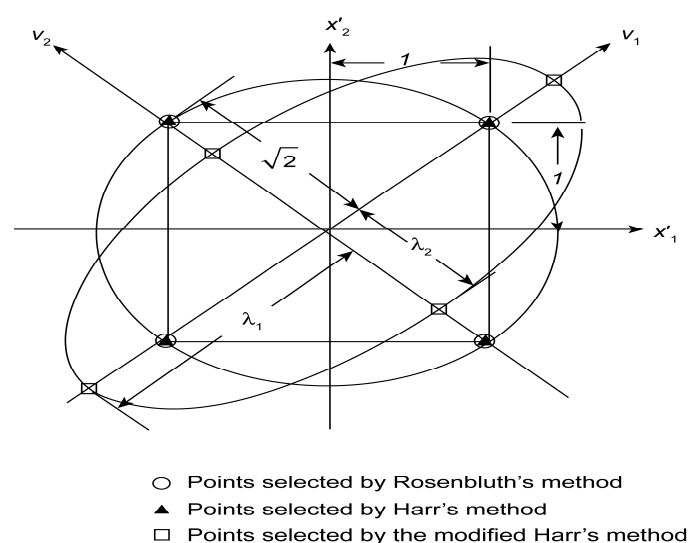


Figure 5. Schematic of the three Point Estimate Methods (PEMs) in a standardized parameter space for a bivariate case.

3.2. Monte Carlo Simulation (MCS)

Monte Carlo simulation (MCS) is a powerful statistical analysis tool and is widely used in both non-engineering fields and engineering fields. It was initially used to solve neutron diffusion problems in atomic bomb work at the Alamos Scientific Laboratory (City, US State abbrev. USA) in 1944. More specifically, MCS can be used in order to describe a given means of propagating (translating) uncertainties in the inputs of a model into uncertainties in the outputs (results) of said model. In principle, if a problem is one with a probabilistic interpretation, MCS can be used to solve it. According to the law of large numbers, for a given stochastic variable, the empirical mean (also known as the sample mean) of a set of independent samples of the variable can be used to approximate the integrals described by the expected value of the variable. MCS is an alternative method of calculating the failure probability that is more versatile than the margin of safety method described earlier. Further explanations of MCS can be found in [12,13].

3.3. Cross Correlation among Parameters

From references (see in Table 3), we knew there was a negative correlation between the rock layer parameter c and ϕ , with its value of $\rho = -0.5 \sim 0$. The research investigated the correlation coefficient $\rho(c, \phi)$ to understand if it would affect the failure probability (P_f).

Table 3. $\rho(c, \phi)$ values.

Parameter	Value	Reference
$\rho(c, \phi)$	−0.2	Leung & Quek (1995) [47].
	−0.3	Baecher & Christian (2003), W. Wang, C. Q. Li, and S. Wang (2011) [48,49].
	−0.5	Low (1997), Li, Zhou, Lu, & Jiang (2009), H.-Z. Li & Low (2010) [7,33,50].

3.4. Probability Density Function (PDF)

For a given continuous stochastic variable, the probability density function (PDF) of that variable is a function that describes the relative probability of the variable occurring at a given point. The integral of the probability density function over the entire space in question is equal to one. The PDF defines the distribution of the stochastic variable and can take many shapes. A convenient probability-distribution type (e.g., normal or lognormal) may be selected, and calibrated with those mean values and standard deviations that are consistent with the engineer's judgment.

4. Results

4.1. Sensitivity Analysis

The research used Excel (version 2017) for sensitivity analysis, respectively calculating the range of the factor of safety both prior to and after the immersion of rock layers in water. The result showed the factor of safety before and after the immersion as 3.04 and 1.53, respectively, consistent with the report from the Ministry of Transportation and Communications (MOTC, 2011) [43]. It proved the spread slope failure model as an appropriate and plausible method for research.

According to the report by the MOTC (2011), the unit weight of rock layers was not affected by water immersion, but it induced reduction in the cohesion c and the friction angle ϕ , weakening the rock layers. Therefore, the research would target the greater variation in cohesion c and its friction angle ϕ , as well as the uncertainty of failure in pre-stressing force T of rock anchor, in order to analyze the factor of safety and sensitivity of slope stability. The univariate and the multi-variate sensitivity analyses are described below.

4.1.1. Univariate Sensitivity Analysis

The experiment design would conduct a univariate sensitivity analysis by setting five equidistant reductions, range of 10–50% in the rock layer parameter cohesion c , friction angle ϕ , and the pre-stressing force T of rock anchor, in order to understand the influences on factor of safety by these variations. The cohesion c value was, respectively, designed as 10 kPa and an average of 59 kPa for in situ tests. As for the friction angle, it was reduced from $\phi = 30^\circ$ to $\phi = 10^\circ$ (an interval of 5°). The designed pre-stressing force of rock anchor was preset at 600 kN. These were tested in 10 samples of five groups to study the sensitivity of factor of safety for the slope (sample design as shown in Table 4). Figures 6 and 7 show the safety factor sensitivity test results. The research discovered that when cohesion $c = 59$ kPa, these factors' sensitivity to the safety of slope as indicated by the factor of safety (FS) ranked in the order of $c > \phi > T$ (see Figure 6). When $c = 10$ kPa, the order of sensitivity to the factor of safety was $\phi > c > T$ (see Figure 7). In addition, the sensitivity of pre-stressing force of the rock anchor was always smaller than the influence by change in rock layer parameter c and ϕ . When c decreased to a threshold, the influence on sensitivity of the factor would be same as ϕ , as seen in Figure 8. In the research, the threshold c value was defined as $C\phi c$. The study found that $C\phi c$ would decrease as ϕ (as shown in Figure 9). From the linear function as Equation (3), it was found that the area above the equation line had the sensitivity $c > \phi$, while the area below would show the opposite, $c < \phi$:

$$C\phi c = 1.032\phi - 1.44, \quad (3)$$

Table 4. Sample design tables for univariate sensitivity analysis.

No.	Parameter	c (kPa)	ϕ ($^\circ$)	T (kN)
1	1	59	30	600
	2	10	30	600
2	1	59	25	600
	2	10	25	600
3	1	59	20	600
	2	10	20	600
4	1	59	15	600
	2	10	15	600
5	1	59	10	600
	2	10	10	600

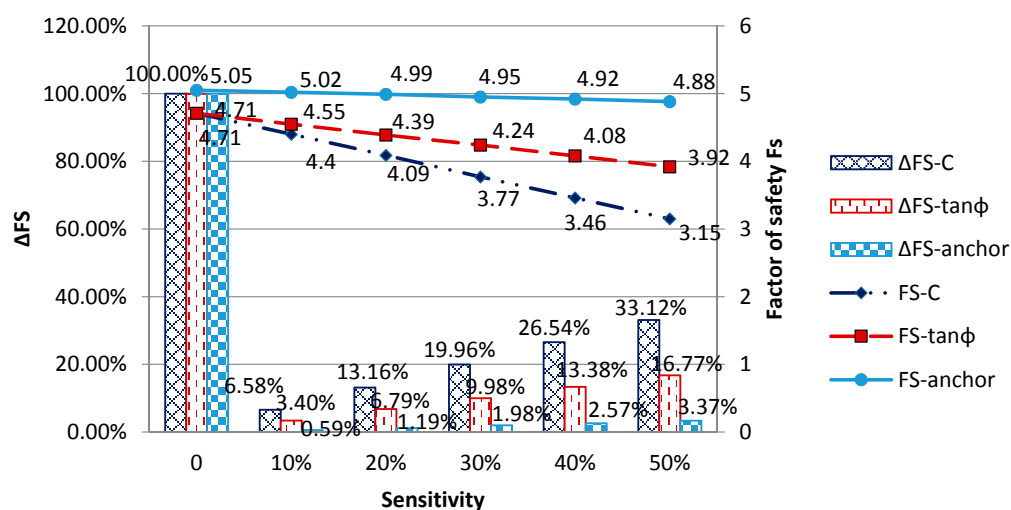


Figure 6. Univariate sensitivity analysis when $c = 59$ kPa and $\phi = 30^\circ$.

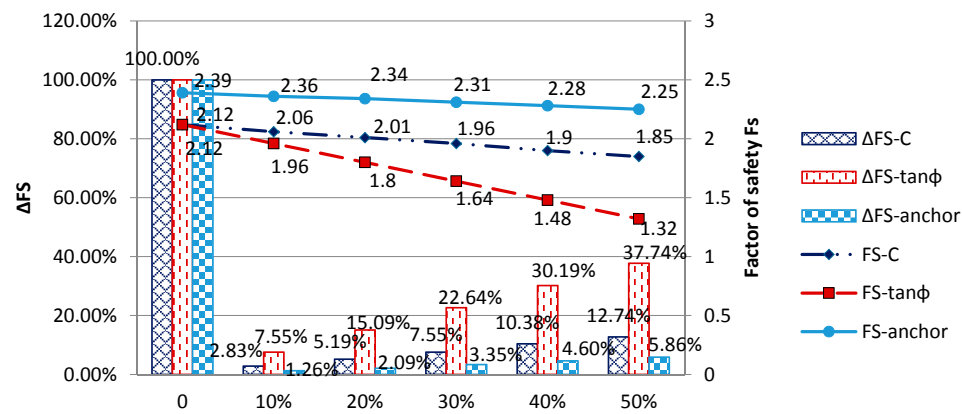
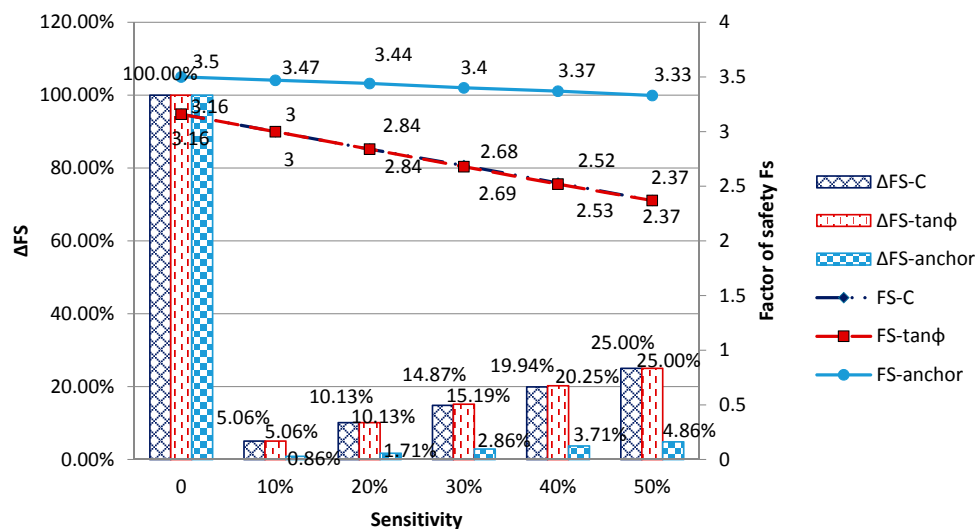
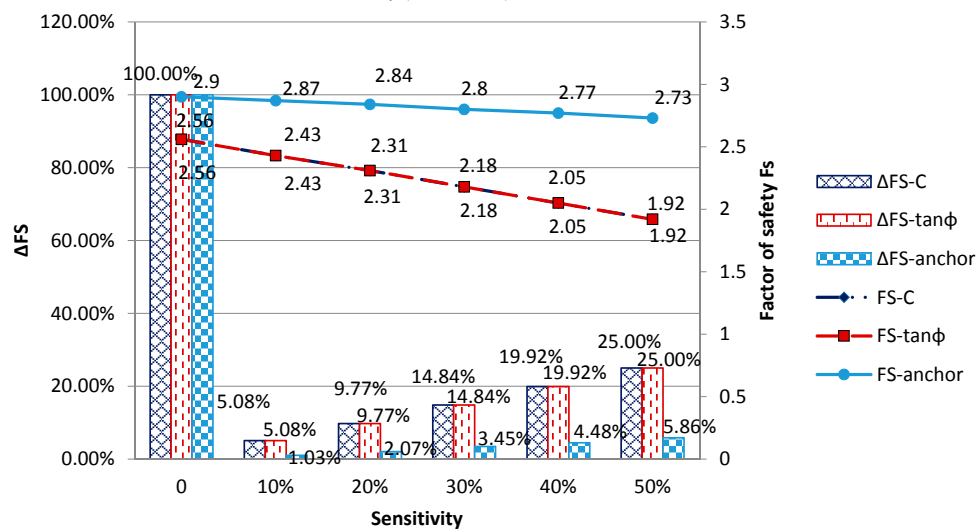


Figure 7. Univariate sensitivity analysis when $c = 10$ kPa and $\phi = 30^\circ$.

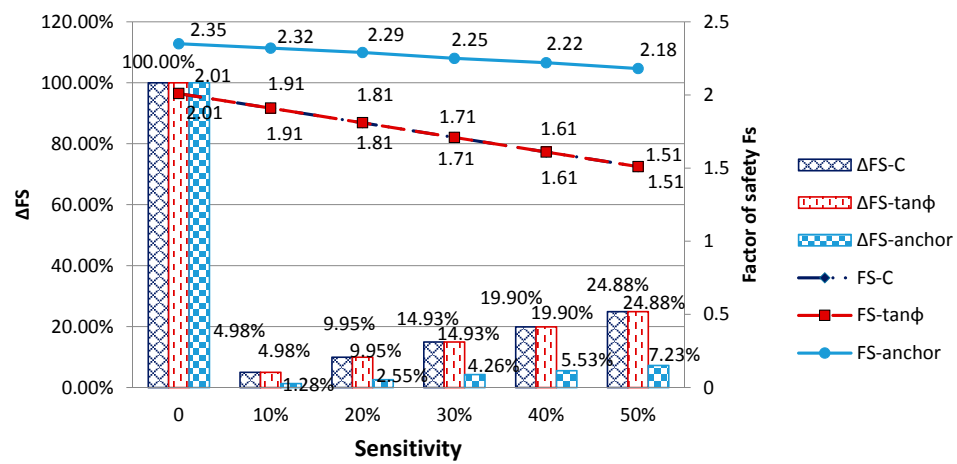


(a) Sensitivity $\phi = c$ when $\phi = 30^\circ$ and $c = 29.7$ kPa

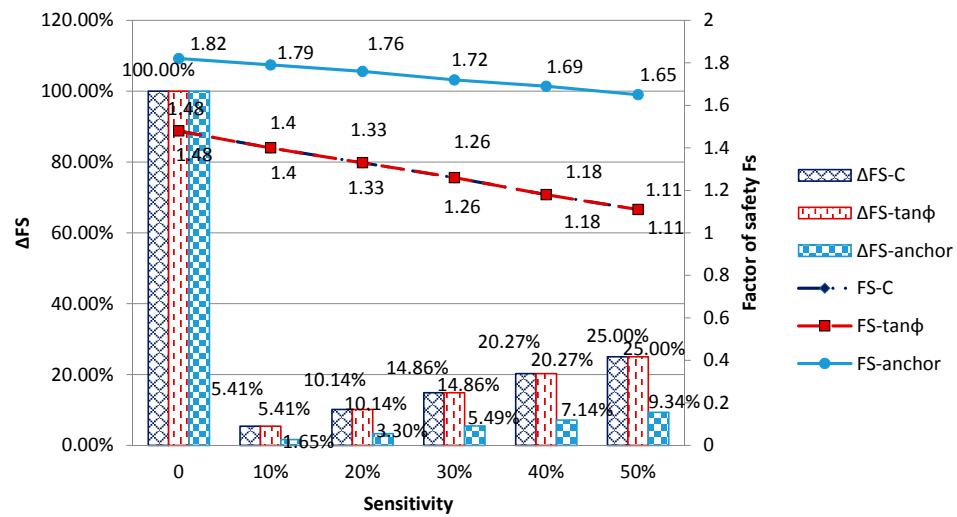


(b) Sensitivity $\phi = c$ when $\phi = 25^\circ$ and $c = 24.2$ kPa

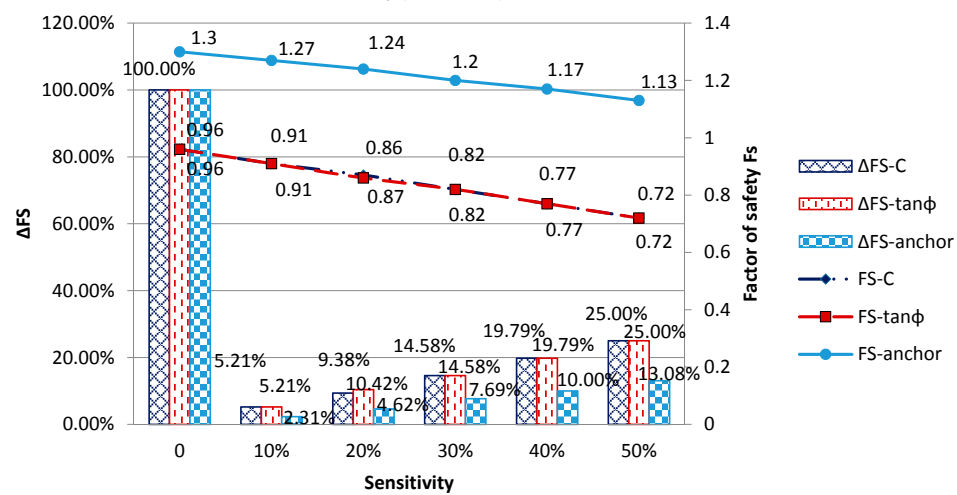
Figure 8. Cont.



(c) Sensitivity $\phi = c$ when $\phi = 20^\circ$ and $c = 19.1$ kPa



(d) Sensitivity $\phi = c$ when $\phi = 15^\circ$ and $c = 14$ kPa



(e) Sensitivity $\phi = c$ when $\phi = 10^\circ$ and $c = 9$ kPa

Figure 8. Sensitivity $\phi = c$ test.

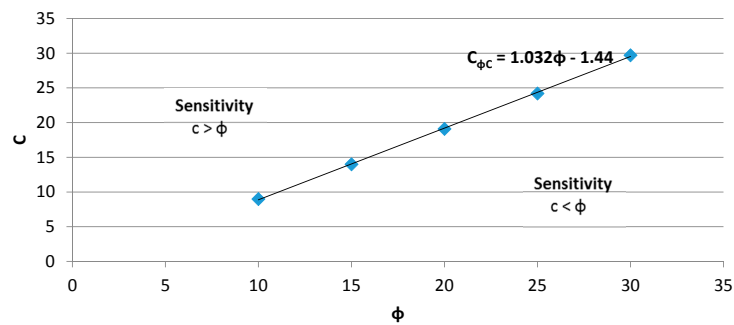


Figure 9. $C_{\phi C}$ linear function.

4.1.2. Multivariate Sensitivity Analysis

Immersion in water would weaken the rock layers. Various parameters would be decreased by such immersion, including the cohesion force c and friction angle ϕ , among others, resulting in lower FS for slope and failure of slope stability. The section would simulate the situation of immersion of slope in water, as both the cohesion force c and friction angle ϕ were decreased, in order to study the influence on the factor of safety. We were transcribed into a 3D distribution chart and contour map for cohesion force c and friction angle ϕ using the MINITAB v15 (see in Figure 10). From the contour map, it was known that when the cohesion force c was reduced to 6 kPa and the friction angle ϕ was reduced below 14° , the FS would become <1 to show instability and failure.

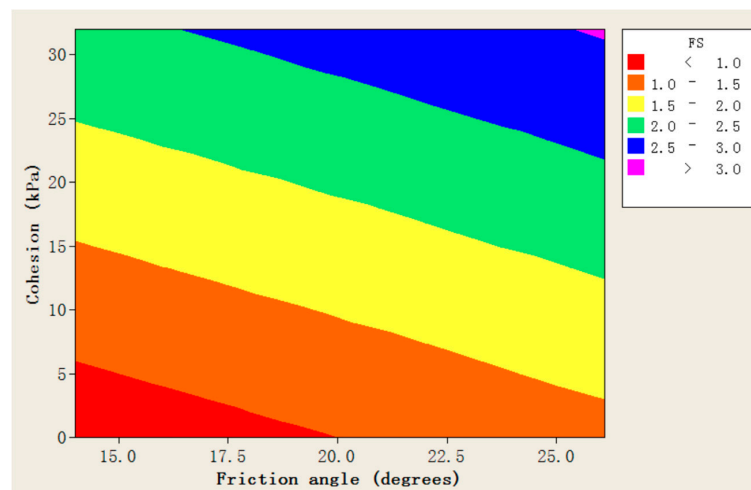


Figure 10. Factor of safety contour map.

4.2. Uncertainty Analysis

The section would use the theory of uncertainty analysis to simulate the landslide case at 3.1 k of the National Freeway No. 3 as a means of establishing a slope model, in order to investigate the slope parameter of rock layers (c , ϕ) and pre-stressing force of rock anchor before and after reinforcement, in order to understand the influence on slope stability by these factor variations. From reference to the in situ drilling test (see in Table 1) by the MOTC (2011), parameters were organized as shown in Tables 5 and 6. The Microsoft Visual Studio 2010 was the system in FORTAN language by the team led by Professor Zhang, Zhe-Hao of the Taipei Technology University. The probability test was based on the three PEMs (RPEM, HPEM and MPEM) and MCS (100,000 sampling counts) under the curve for both the normal and lognormal PDF distributions. It aims to estimate the FS and P_f prior to and after the water immersion and rock anchor reinforcement. We used the MCS to verify the accuracy of PEM. The result was described below:

Table 5. Fix parameters.

Fix Parameters	Value
Height of slope, H (M)	25
Angle of slip surface, θ ($^{\circ}$)	15
Angle of dip, β ($^{\circ}$)	20
Number of anchors/layer	3
Inclined angle of anchor, δ ($^{\circ}$)	20
Horizontal spacing of anchor, S (m)	2.6

Table 6. Variation parameters.

Parameter	Mean	STD. DEV.	Distribution	Remarks
γ (kN/m ³)	22.9	0.11	(1) Normal distribution (2) Log-normal distribution	
C_p (kN/m ²)	2.8–32		Uniform distribution	Prior to immersion (peak strength)
C_r (kN/m ²)	0		Constant	After immersion (residual strength)
ϕ_p ($^{\circ}$)	26.1	2.23	(1) Normal distribution (2) Log-normal distribution	Prior to immersion (peak strength)
ϕ_r ($^{\circ}$)	19.95	3.62	(1) Normal distribution (2) Log-normal distribution	After immersion (residual strength)
T (kN)	767	153	(1) Normal distribution (2) Log-normal distribution	

If the test was conducted without rock anchor reinforcement, there was no significant variation in the FS and Pf with each probability estimation method (see in Tables 7 and 8). Before the water immersion $FS \cong 2.27 \gg 1$ and $Pf = 0.34\%$ (safe), the FS was greatly reduced to 1 and the original slope failure rate could be as high as 50% (immediate failure), the nature slope requiring immediate stabilization measures (see in Figure 11).

Table 7. Probability estimation methods used to assess factor of safety.

(a) Normal Distribution								
Method			$\rho = 0$		$\rho = -0.25$		$\rho = -0.5$	
			Before Immersion	After Immersion	Before Immersion	After Immersion	Before Immersion	After Immersion
RPEM	MEAN	×	2.2720	1.0018	2.2720	1.0018	2.2720	1.0018
		☑	2.6703	1.4000	2.6703	1.4000	2.6703	1.4000
	STD. DEV.	×	0.4693	0.1968	0.4366	0.1968	0.4011	0.1968
HPEM	MEAN	×	2.2721	1.0018	2.2721	1.0018	2.2721	1.0018
		☑	2.6703	1.4000	2.6703	1.4000	2.6703	1.4000
	STD. DEV.	×	0.4680	0.1977	0.4351	0.1970	0.3996	0.1970
MPEM	MEAN	×	2.2721	1.0018	2.2721	1.0018	2.2721	1.0018
		☑	2.6703	1.4000	2.6703	1.4000	2.6703	1.4000
	STD. DEV.	×	0.4680	0.1977	0.4350	0.1970	0.3995	0.1971
MCS	MEAN	×	2.2721	1.0021	2.2723	1.0016	2.2723	1.0015
		☑	2.6699	1.3919	2.6700	1.3918	2.6702	1.3918
	STD. DEV.	×	0.4696	0.1977	0.4362	0.1982	0.4005	0.1981
		☑	0.4788	0.2261	0.4460	0.2260	0.4115	0.2261

Table 7. Cont.

(b) Log-Normal Distribution								
Method			$\rho = 0$		$\rho = -0.25$		$\rho = -0.5$	
			Before Immersion	After Immersion	Before Immersion	After Immersion	Before Immersion	After Immersion
RPEM	MEAN	✗	2.2721	1.0020	2.2721	1.0020	2.2721	1.0020
		☑	2.6703	1.4002	2.6703	1.4002	2.6703	1.4002
	STD. DEV.	✗	0.4695	0.1994	0.4368	0.1994	0.4014	0.1994
		☑	0.4783	0.2155	0.4477	0.2155	0.4147	0.2155
HPEM	MEAN	✗	2.2721	1.0018	2.2721	1.0018	2.2721	1.0018
		☑	2.6703	1.4000	2.6703	1.4000	2.6703	1.4000
	STD. DEV.	✗	0.4680	0.1977	0.4351	0.1970	0.3996	0.1970
		☑	0.4769	0.2142	0.4446	0.2134	0.4099	0.2134
MPEM	MEAN	✗	2.2721	1.0020	2.2721	1.0019	2.2721	1.0019
		☑	2.6703	1.4003	2.6703	1.4001	2.6703	1.4002
	STD. DEV.	✗	0.4681	0.1994	0.4349	0.1974	0.3993	0.1984
		☑	0.4770	0.2169	0.4444	0.2143	0.4094	0.2156
MCS	MEAN	✗	2.2721	1.0015	2.2723	1.0012	2.2723	1.0011
		☑	2.6698	1.3785	2.6700	1.3788	2.6702	1.3787
	STD. DEV.	✗	0.4698	0.2005	0.4362	0.2008	0.4005	0.2006
		☑	0.4789	0.2456	0.4459	0.2450	0.4114	0.2455

RPEM: Rosenblueth point estimate method; HPEM: Harr point estimate method; MPEM: Modified Harr point estimate method; MCS: Monte Carlo Simulation; ✗: Without anchor force; ☑: With anchor force.

Table 8. Probability estimation methods used to assess failure probability.

Method			$\rho = 0$		$\rho = -0.25$		$\rho = -0.5$	
			Before Immersion	After Immersion	Before Immersion	After Immersion	Before Immersion	After Immersion
RPEM	Normal	✗	0.34%	49.64%	0.18%	49.64%	0.08%	49.64%
		☑	0.02%	3.03%	0.01%	3.03%	0.00%	3.03%
	Log-normal	✗	0.34%	49.60%	0.18%	49.60%	0.08%	49.60%
		☑	0.02%	3.17%	0.01%	3.17%	0.00%	3.17%
HPEM	Normal	✗	0.33%	49.64%	0.17%	49.64%	0.07%	49.64%
		☑	0.02%	3.09%	0.01%	3.04%	0.00%	3.04%
	Log-normal	✗	0.33%	49.64%	0.17%	49.64%	0.07%	49.64%
		☑	0.02%	3.09%	0.01%	3.04%	0.00%	3.04%
MPEM	Normal	✗	0.33%	49.64%	0.17%	49.64%	0.07%	49.64%
		☑	0.02%	3.09%	0.01%	3.04%	0.00%	3.06%
	Log-normal	✗	0.33%	49.60%	0.17%	49.62%	0.07%	49.62%
		☑	0.02%	3.25%	0.01%	3.10%	0.00%	3.17%
MCS	Normal	✗	0.34%	49.58%	0.18%	49.68%	0.07%	49.70%
		☑	0.02%	4.15%	0.01%	4.15%	0.00%	4.16%
	Log-normal	✗	0.34%	49.70%	0.18%	49.76%	0.07%	49.78%
		☑	0.02%	6.16%	0.01%	6.10%	0.00%	6.15%

RPEM: Rosenblueth point estimate method; HPEM: Harr point estimate method; MPEM: Modified Harr point estimate method; MCS: Monte Carlo Simulation; ✗: Without anchor force; ☑: With anchor force.

In the research, we also analyzed the situation of rock anchor reinforcement, which could effectively improve the factor of safety by 0.39. However, the measure of rock anchor reinforcement still posed the uncertainty of losing pre-stressing force. The study would include the variation in loss of pre-stressing force of rock anchor as a factor for investigation. It was found that after rock anchor reinforcement, under water immersion, the P_f could be reduced from 50 to 3–4%, while it could significantly improve the slope stability and reliability (see in Figure 12).

The study would set the correlation coefficient $\rho = (0, -0.25, -0.5)$ as the test parameter. The test result proved correlation coefficient ρ before and after water immersion would not affect the average

FS value (mean), but would certainly affect the failure probability (P_f). Before water immersion, due to cohesion force $c > 0$ and larger absolute value of ρ (c, ϕ), the failure probability (P_f) was smaller (see in Figure 13). After water immersion, the rock layers were weakened, as cohesion force c was reduced to 0 kPa and regardless of ρ (c, ϕ) value, the failure probability (P_f) would not change.

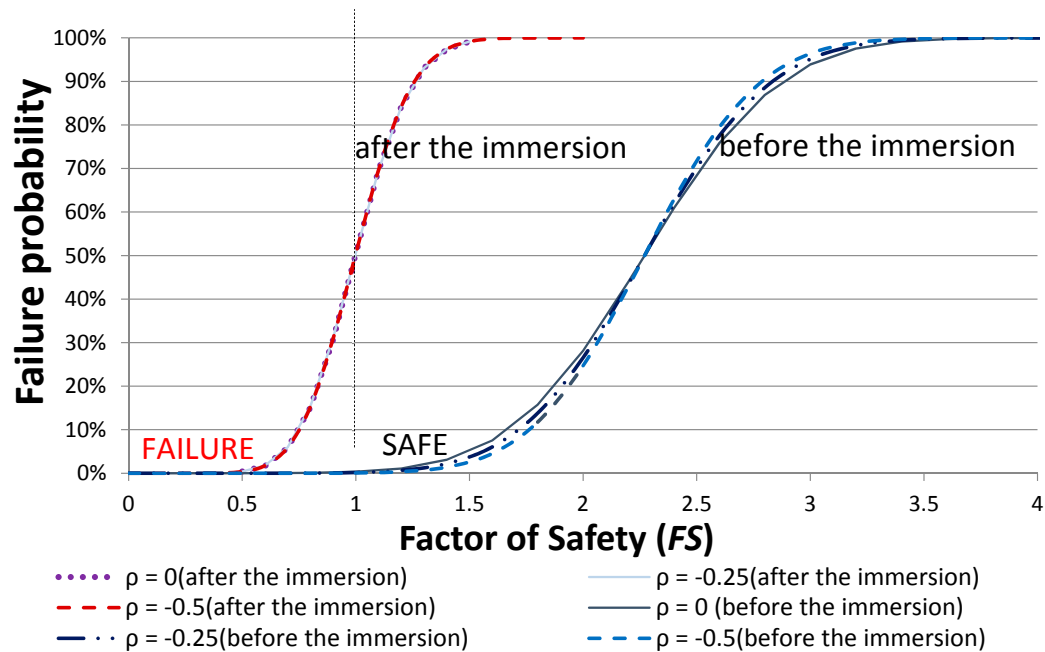


Figure 11. Failure probability before and after immersion (without anchor).

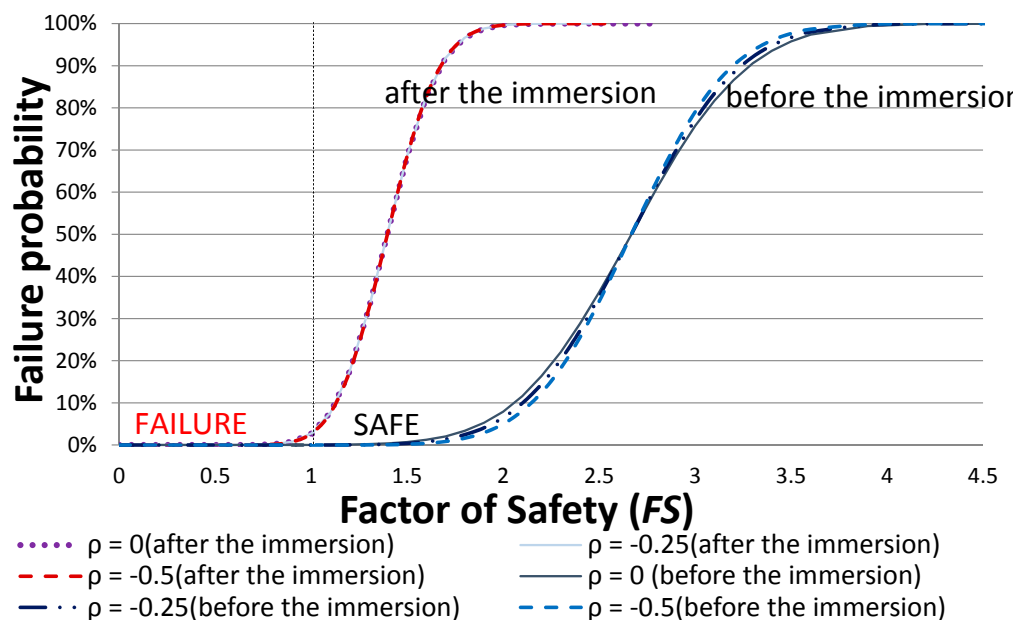


Figure 12. Failure probability before and after immersion (with anchor).

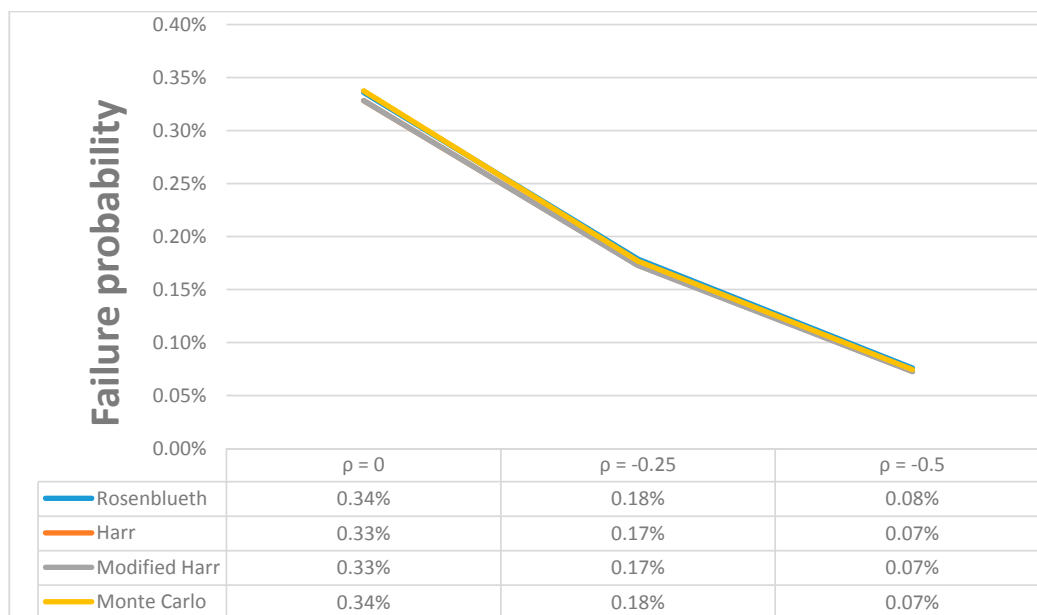


Figure 13. Relationship between correlation coefficient (ρ) and failure probability (P_f).

The case study uses the normal distribution and lognormal distribution, which are the most commonly-used ones in geotechnical applications. The study of this aspect is summarized in Table 8. PEM uses normal distribution and lognormal distribution, without rock anchor and $\rho = 0$ as an example, before water immersion, $P_f = 0.33\text{--}0.34\%$ (with normal and lognormal distribution). The result indicates no significant difference. Calculated with MCS verification, $P_f = 0.34\%$ (with normal and lognormal distribution), the results are consistent. Besides after water immersion, the results reveal the following numbers $P_f = 49.60\text{--}49.64\%$ (PEM with normal and lognormal distribution), $P_f = 49.58\%$ (MCS—normal distribution) and $P_f = 49.70\%$ (MCS—lognormal distribution). It shows that the three PEMs and MCS under the curve for both the normal and lognormal PDF distributions have the same result.

5. Discussion

The research used the slope failure case at 3K+100 location on the National Highway No. 3 as a reference to establish a slope failure model. With the sensitivity analysis and probability estimation method, in consideration of the variation of the rock parameters and anchor force, together with investigation of the correlation coefficient ρ and both the normal and lognormal PDF distributions, we conducted research on their effect on the FS and P_f . Thus, the conclusions were stated below:

1. From the univariate sensitivity test result, the sensitivity to the pre-stressing force of rock anchor T was significantly less than the influence by variation in the cohesion force c and friction angle ϕ . When c decreased to a threshold, the influence on sensitivity of the factor would be the same as friction angle ϕ . The threshold c value was defined as a linear function $C_{\phi c} = 1.032\phi - 1.44$. It was found that the area above the equation line had the sensitivity $c > \phi$, while the area below would show the opposite, $c < \phi$. The results of the sensitivity analysis provide engineers with an important factor in understanding the impact of the slope collapse. In the future, in determining the failure of the slope system, it is possible to obtain important factors in this result and to make relevant improvements or reinforcement measures.
2. From the multi-variate sensitivity test, it was known that when the cohesion force c was reduced to 6 Kpa and the friction angle ϕ was reduced below 14° , the slope factor of safety (FS) < 1 and started to show instability and failure. The results show that, consistent with the report from the MOTC (2011), it is shown that the slope failure model established in this study can reasonably simulate the slope failure.

3. Without considering the rock anchor reinforcement, the failure probability rate before water immersion $FS \cong 2.27 \gg 1$ and $Pf = 0.34\%$ (safe), even though $FS \cong 1$ (immediate failure) was seen after water immersion. The slope was near the threshold of failure and the rate was as high as 50%. After rock anchor reinforcement, the FS was improved by 0.39 and the Pf was reduced to 3–4%, significantly improving the slope stability and reliability. However, the rock anchor has a useful life, and it requires frequent inspections and maintenance, once the loss of reinforcement function occurs, the slope system will be destroyed, for similar reasons as for the destruction in the study case. Our results showed that the slope stability assessment and FS calculations involve many variables. Probability analysis takes into account rock formation parameters and rock anchor variability, calculates the failure probability and therefore offers very significant benefits over traditional limit equilibrium methods in the analysis of highly variable soils.
4. The correlation coefficient of these parameters $\rho(c, \phi)$ would not affect the average value for the FS , but would affect that for the Pf . When the absolute value of $\rho(c, \phi)$ increased, the Pf decreased. However the results were almost the same, thus proving a simplification of the calculation.
5. The three PEMs and MCS under the curve for both the normal and lognormal PDF distributions are almost the same. Therefore, they bring about the outcome that, in geotechnical applications, we can only use the normal distribution.

6. Conclusions

This paper used the dip-slope failure at Section 3.1 K of Taiwan Formosa Freeway (Freeway No. 3) as a case study. Our study target was to frame a slope model consistent with field conditions in an attempt to explore the variations of slope safety factor and variability of rock slope parameters (c, ϕ) and anchor force (T) before and after immersion and weakening of slope rocks. First, we used the sensitivity analysis to explore the impact of the uncertainty or variability of the input parameter values on the safety factor; second, three different PEMs (RPEM, HPEM and MPEM) were used to study the effect of parameter uncertainty on slope stability, and MCS was used to check the accuracy. The results show that the traditional slope stability analysis is not good enough; moreover, the importance of the probability analysis is illustrated.

The case of the disaster is mainly and typically slope sliding. According to the characteristics of the disaster, the sliding surface of the sliding slope is weakened by the groundwater infiltration. The destruction has reached a critical slip before the situation, and rock anchor components have an obvious corrosion phenomenon, will gradually reduce the tensile strength of anchor and slope safety factor, but also cause the slope system failure in a short time. In this study, the probability analysis also illustrates this failure mechanism ($Pf = 50\%$). It can be seen that the variations of slope safety factor and variability of rock slope parameters (c, ϕ) and anchor force (T) have great influence on slope safety.

Author Contributions: Chia-Pang Cheng simulations, analyzed application results, and wrote the manuscript; Shong-Loong Chen offered useful suggestions for the manuscript preparation and writing.

Conflicts of Interest: The authors declare no conflict of interest.

References

1. Wyllie, D.C.; Mah, C.W. *Rock Slope Engineering*, 4th ed.; Taylor & Francis: Abingdon, UK, 2007.
2. Phoon, K.K. Towards Reliability-Based Design for Geotechnical Engineering. Available online: http://www.eng.nus.edu.sg/civil/people/cvepkk/Special_KGS_2004.pdf (accessed on 18 August 2017).
3. Wu, X.Z. Probabilistic slope stability analysis by a copula-based sampling method. *Comput. Geosci.* **2013**, *17*, 739–755. [CrossRef]
4. Alonso, E.E. Discussion: Risk analysis of slopes and its application to slopes in Canadian sensitive clays. *Géotechnique* **1977**, *27*, 254–258. [CrossRef]
5. Canada Centre for Mineral and Energy Technology; Mining Research Laboratories. *Pit Slope Manual*; Minerals Research Program, Mining Research Laboratories: Ottawa, QC, Canada, 1978.

6. Fredlund, D.G.; Krahn, J. Comparison of slope stability methods of analysis. *Can. Geotech. J.* **1977**, *14*, 429–439. [[CrossRef](#)]
7. Low, B.K. Reliability analysis of rock wedges. *J. Geotech. Geoenviron. Eng.* **1997**, *123*, 498–505. [[CrossRef](#)]
8. Matsuo, M.; Kuroda, K. Probabilistic approach to design of embankments. *Soils Found.* **1974**, *14*. [[CrossRef](#)]
9. Wu, T.H.; Kraft, L.M. Safety analysis of slopes. *J. Soil Mech. Found. Div.* **1970**, *96*, 609–630.
10. Yucemen, M.S.; Tang, W.H.; Ang, A.S. *A Probabilistic Study of Safety and Design of Earth Slopes*; University of Illinois at Urbana: Champaign, IL, USA, 1973; pp. 1–204.
11. Schmidt, J.; Dikau, R. Modeling historical climate variability and slope stability. *Geomorphology* **2004**, *60*, 433–447. [[CrossRef](#)]
12. Zhang, L.L.; Zuo, Z.B.; Ye, G.L.; Jeng, D.S.; Wang, J.H. Probabilistic parameter estimation and predictive uncertainty based on field measurements for unsaturated soil slope. *Comput. Geotech.* **2013**, *48*, 72–81. [[CrossRef](#)]
13. Li, D.Q.; Xiao, T.; Cao, Z.J.; Zhou, C.B.; Zhang, L.M. Enhancement of random finite element method in reliability analysis and risk assessment of soil slopes using Subset Simulation. *Landslides* **2016**, *13*, 293–303. [[CrossRef](#)]
14. Kaur, A.; Sharma, R.K. Slope stability analysis techniques: A review. *Int. J. Eng. Appl. Sci. Technol.* **2016**, *1*, 52–57.
15. El-Ramly, H.; Morgenstern, N.R.; Cruden, D.M. Lodalén slide: A probabilistic assessment. *Can. Geotech. J.* **2006**, *43*, 956–968. [[CrossRef](#)]
16. Babanouri, N. Investigating a potential reservoir landslide and suggesting its treatment using limit-equilibrium and numerical methods. *J. Mt. Sci.* **2017**, *14*, 432–441. [[CrossRef](#)]
17. Iovine, G.G.; Greco, R.; Gariano, S.L.; Pellegrino, A.D.; Terranova, O.G. Shallow-landslide susceptibility in the Costa Viola with considerations on the role of causal factors. *Nat. Hazards* **2014**, *73*, 111–136. [[CrossRef](#)]
18. Jaiswal, P.; van Westen, C.J.; Jetten, V. Quantitative landslide hazard assessment along a transportation corridor in southern India. *Eng. Geol.* **2010**, *116*, 236–250. [[CrossRef](#)]
19. Wu, X.Z. Assessing the correlated performance functions of an engineering system via probabilistic analysis. *Struct. Saf.* **2015**, *52*, 10–19. [[CrossRef](#)]
20. Malkawi, A.I.H.; Hassan, W.F.; Abdulla, F.A. Uncertainty and reliability analysis applied to slope stability. *Struct. Saf.* **2000**, *22*, 161–187. [[CrossRef](#)]
21. Wu, X.Z. Implementing statistical fitting and reliability analysis for geotechnical engineering problems in R. *Georisk* **2016**, *11*, 173–188. [[CrossRef](#)]
22. Xiao, Z.Q.; Huang, J.; Wang, Y.J.; Xu, C.Y.; Huan, X.I.A. Random reliability analysis of gravity retaining wall structural system. In Proceedings of the International Conference on Mechanics and Civil Engineering (ICMCE 2014), Wuhan, China, 13–14 December 2014; pp. 199–204.
23. Ji, J.; Low, B.K. Stratified response surfaces for system probabilistic evaluation of slopes. *J. Geotech. Geoenviron. Eng.* **2012**, *138*, 1398–1406. [[CrossRef](#)]
24. Li, L.; Chu, X. Multiple response surfaces for slope reliability analysis. *Int. J. Numer. Anal. Meth. Geomech.* **2015**, *39*, 175–192. [[CrossRef](#)]
25. Cho, S.E. Probabilistic stability analyses of slopes using the ANN-based response surface. *Comput. Geotech.* **2009**, *36*, 787–797. [[CrossRef](#)]
26. Wang, Y.; Cao, Z.; Au, S.K. Practical reliability analysis of slope stability by advanced Monte Carlo simulations in a spreadsheet. *Can. Geotech. J.* **2011**, *48*, 162–172. [[CrossRef](#)]
27. Santoso, A.M.; Phoon, K.K.; Quek, S.T. Effects of soil spatial variability on rainfall-induced landslides. *Comput. Struct.* **2011**, *89*, 893–900. [[CrossRef](#)]
28. Eldred, M.S. Recent advances in non-intrusive polynomial chaos and stochastic collocation methods for uncertainty analysis and design. In Proceedings of the 50th AIAA/ASME/ASCE/AHS/ASC Structures, Structural Dynamics, and Materials Conference, Palm Springs, CA, USA, 4–7 May 2009.
29. Xiu, D. Efficient collocational approach for parametric uncertainty analysis. *Commun. Comput. Phys.* **2006**, *2*, 293–309.
30. Upadhyay, R.R.; Ezekoye, O.A. Treatment of design fire uncertainty using quadrature method of moments. *Fire Saf. J.* **2008**, *43*, 127–139. [[CrossRef](#)]
31. Marchisio, D.L.; Vigil, R.D.; Fox, R.O. Implementation of the quadrature method of moments in CFD codes for aggregation—breakage problems. *Chem. Eng. Sci.* **2003**, *58*, 3337–3351. [[CrossRef](#)]

32. Tobutt, D.C. Monte carlo simulation methods for slope stability. *Comput. Geosci.* **1982**, *8*, 199–208. [CrossRef]
33. Li, D.; Zhou, C.; Lu, W.; Jiang, Q. A system reliability approach for evaluating stability of rock wedges with correlated failure modes. *Comput. Geotech.* **2009**, *36*, 1298–1307. [CrossRef]
34. Mbarka, S.; Baroth, J.; Ltifi, M.; Hassis, H.; Darve, F. Reliability analyses of slope stability: Homogeneous slope with circular failure. *Eur. J. Environ. Civ. Eng.* **2010**, *14*, 1227–1257. [CrossRef]
35. Huang, J.; Griffiths, D.V.; Fenton, G.A. System reliability of slopes by RFEM. *Soils Found.* **2010**, *50*, 343–353. [CrossRef]
36. Xin, C.; Chongshi, G. Risk analysis of gravity dam instability using credibility theory Monte Carlo simulation model. *SpringerPlus* **2016**, *5*. [CrossRef] [PubMed]
37. Harr, M.E. Probabilistic estimates for multivariate analyses. *Appl. Math. Model.* **1989**, *13*, 313–318. [CrossRef]
38. Abbaszadeh, M.; Shahriar, K.; Sharifzadeh, M.; Heydari, M. Uncertainty and reliability analysis applied to slope stability: A case study from sungun copper mine. *Geotech. Geol. Eng.* **2011**, *29*, 581–596. [CrossRef]
39. Wang, J.P.; Huang, D. RosenPoint: A Microsoft Excel-based program for the Rosenblueth point estimate method and an application in slope stability analysis. *Comput. Geosci.* **2012**, *48*, 239–243. [CrossRef]
40. Ahmadabadi, M.; Poisel, R. Probabilistic analysis of rock slopes involving correlated non-normal variables using point estimate methods. *Rock Mech. Rock Eng.* **2016**, *49*, 909–925. [CrossRef]
41. Christian, J.T.; Baecher, G.B. The point-estimate method with large numbers of variables. *Int. J. Numer. Anal. Methods Geomech.* **2002**, *26*, 1515–1529. [CrossRef]
42. Chen, S.L.; Cheng, C.P.; Gui, M.W. Sensitivity and uncertainty analyses of the translational slide at the Cidu section, 3.1 k of the Taiwan Formosan freeway. In Proceedings of the Fourth Geo-China International Conference, Shandong, China, 25–27 July 2016; pp. 81–89.
43. Ministry of Transportation and Communications R.O.C. Summary Report of Investigation of Reasons for Taiwan Freeway 3 (Formosan Freeway Cidu Section) 3.1k Landslide. Available online: <https://drive.google.com/file/d/0B5-uoBhbSoMOT00wVHEydjBXV0E/view> (accessed on 18 August 2017). (In Chinese)
44. Hoek, E.; Bray, J. *Rock Slope Engineering*, 3rd ed.; Institution of Mining and Metallurgy: London, UK, 1981.
45. Chang, C.-H.; Tung, Y.-K.; Yang, J.-C. Evaluation of probability point estimate methods. *Appl. Math. Model.* **1995**, *19*, 95–105.
46. Rosenblueth, E. Point estimates for probability moments. *Proc. Natl. Acad. Sci. USA.* **1975**, *72*, 3812–3814. [CrossRef] [PubMed]
47. Quek, S.T.; Leung, C.F. Reliability-based stability analysis of rock excavations. *Int. J. Rock Mech. Min. Sci. Geomech. Abstr.* **1995**, *32*, 617–620. [CrossRef]
48. Baecher, G.B.; Christian, J.T. *Reliability and Statistics in Geotechnical Engineering*; Wiley: Chichester, UK, 2003; Volume 1.
49. Wang, W.; Li, C.Q.; Wang, S. Slope instability risk analysis in earth dams considering uncertain factors. *Appl. Mech. Mater.* **2011**, *117–119*, 1475–1478. [CrossRef]
50. Li, H.Z.; Low, B.K. Reliability analysis of circular tunnel under hydrostatic stress field. *Comput. Geotech.* **2010**, *37*, 50–58. [CrossRef]

